Tellus (2007), 59A, 355–366
Printed in Singapore.

TELLUS

An efficient method for recovering Lyapunov vectors from singular vectors

By CHRISTOPHER L. WOLFE* and ROGER M. SAMELSON, *College of Oceanic and Atmospheric Sciences, Oregon State University, 104 COAS Admin. Bldg., Corvallis, OR 97331-5503, USA*

(Manuscript received 24 May 2006; in final form 2 February 2007)

ABSTRACT

Lyapunov vectors are natural generalizations of normal modes for linear disturbances to aperiodic deterministic flows and offer insights into the physical mechanisms of aperiodic flow and the maintenance of chaos. Most standard techniques for computing Lyapunov vectors produce results which are norm-dependent and lack invariance under the linearized flow (except for the leading Lyapunov vector) and these features can make computation and physical interpretation problematic. An efficient, norm-independent method for constructing the n most rapidly growing Lyapunov vectors from $n - 1$ leading forward and n leading backward asymptotic singular vectors is proposed. The Lyapunov vectors so constructed are invariant under the linearized flow in the sense that, once computed at one time, they are defined, in principle, for all time through the tangent linear propagator. An analogous method allows the construction of the n most rapidly decaying Lyapunov vectors from n decaying forward and $n - 1$ decaying backward singular vectors. This method is demonstrated using two low-order geophysical models.

1. Introduction

Geophysical fluid flows often exhibit complex and apparently random behaviour. One compelling explanation for this apparent randomness is that small errors in the initial, boundary, and forcing conditions are amplified by instabilities of the fluid motions. This is an example the so-called sensitive dependence on initial conditions of nonlinear dynamical systems. Several techniques have been developed to quantify linear disturbance growth in systems subject to sensitive dependence on initial conditions, including the traditional normal-mode instability theories of fluid dynamics (e.g. Drazin and Reid, 2004), Lyapunov vectors from dynamical systems theory (Oseledec, 1968; Eckmann and Ruelle, 1985) and singular vectors from ensemble forecasting (Lorenz, 1965; Farrell, 1989; Buizza and Palmer, 1995; Buizza et al., 2005).

Normal modes, in the simplest conceptions, are linear disturbances with a fixed spatial structure, which grow at a fixed exponential rate. An important property of normal modes is that they are invariant under the linearized flow; that is, once they are determined at one time, they are determined for all past and future times by the linear propagator. Singular vectors, by contrast, optimize disturbance growth in a specified norm over a specified time-interval, and their spatial structure is generally time-dependent. In contrast to normal modes, singular vectors are generally not invariant under the linearized flow and, in fact, have little dynamical meaning for times outside their optimization interval. Lyapunov vectors, which have generally received less attention in the literature than Lyapunov exponents, are the time-dependent spatial structures associated with the corresponding Lyapunov exponents, which are in turn the asymptotic exponential growth rates of linear disturbances in general time-dependent flows. The definition of the Lyapunov vectors given in the literature varies depending on the application. We focus on a norm-independent definition of the Lyapunov vectors, which emphasizes their connection to normal modes and renders them invariant under the linearized flow.

We present an efficient, norm-independent method for constructing Lyapunov vectors from asymptotic singular vectors. This method generalizes and improves on similar methods given by Legras and Vautard (1996) and Trevisan and Pancotti (1998). Previous methods required knowledge of $N + 1$ asymptotic singular vectors, where N is the total number of degrees of freedom in the system. In contrast, the method proposed here requires only $2n - 1$ singular vectors to compute n Lyapunov vectors. The method is demonstrated using two low-order geophysical models. The format of the paper is as follows: We review the definitions of, and connections among, singular vectors, Lyapunov vectors, and normal modes in Section 2. In Section 3, we present the method for constructing Lyapunov vectors from singular vectors. Two numerical examples, which demonstrate the

*Correspondence.
e-mail: clwolfe@ucsd.edu
Current affiliation: Scripps Institution of Oceanography
DOI: 10.1111/j.1600-0870.2007.00234.x

method, are presented in Section 4. Finally, Section 5 contains a discussion of some of the practical implications of the method developed in Section 3.

2. Definitions

2.1. Dynamical system and propagator

Consider a flow, which, when discretized, satisfies the autonomous N-dimensional dynamical system

$$\dot{\boldsymbol{x}} = \mathbf{F}(\boldsymbol{x}). \tag{1}$$

In general, N is very large. The evolution of infinitesimal disturbances $\boldsymbol{y}$ to the flow $\boldsymbol{x}$ is governed by the tangent linearization of eq. (1)

$$\dot{\boldsymbol{y}} = \mathbf{A}[\boldsymbol{x}(t)]\,\boldsymbol{y} \tag{2}$$

where

$$\mathbf{A}[\boldsymbol{x}(t)] = \frac{\partial \mathbf{F}[\boldsymbol{x}(t)]}{\partial \boldsymbol{x}}. \tag{3}$$

The propagator $\mathcal{L}(t_2, t_1)$ is the matrix that takes solutions of eq. (2) at time t_1 to solutions of eq. (2) at time t_2. It can be represented as

$$\mathcal{L}(t_2, t_1) = \mathbf{Z}(t_2)\mathbf{Z}(t_1)^{-1}, \tag{4}$$

where $\mathbf{Z}$ is a fundamental solution matrix for eq. (2).

2.2. Normal modes

The traditional definition of normal modes depends on the time dependence of the flow and thus on the time dependence of the matrix $\mathbf{A}$ in eq. (2). If the flow is stationary, the normal modes and their exponential growth rates are simply the eigenvectors and eigenvalues of $\mathbf{A}$, respectively. These normal modes are norm-independent disturbances with fixed spatial structure whose asymptotic stability is determined by the corresponding growth rate. A very useful property of normal modes is that they are often physically meaningful and facilitate the interpretation of flow instability. The normal modes will be orthogonal in a given norm if $\mathbf{A}$ is normal (i.e. it commutes with its adjoint) in that norm. Stationary normal modes are clearly invariant under the linearized flow, described by the constant matrix $\mathbf{A}$, since they are the eigenvectors of this matrix.

If the flow is time-periodic with period T, the normal modes are Floquet vectors: the eigenvectors of the one-period propagator $\mathcal{L}(t+T, t)$ (see, e.g. Coddington and Levinson, 1955). The asymptotic stability of the Floquet vectors is determined by the corresponding Floquet exponents, which are the logarithms of the eigenvalues of $\mathcal{L}(t+T, t)$. The Floquet vectors consist of a time-periodic structure function multiplying a part, which grows or decays exponentially at the rate given by the Floquet exponent. A complete set of Floquet vectors $\mathbf{F}(t)$ represents a fundamental matrix solution to (2), allowing the propagator to be written

$$\mathcal{L}(t_2, t_1) = \mathbf{F}(t_2)\mathbf{F}(t_1)^{-1}, \tag{5}$$

for any two times t_1, t_2, which shows that Floquet vectors are invariant under the linearized flow and can, in principle, be defined for all time from a single eigenvalue problem. Like stationary normal modes, Floquet vectors often have compelling physical interpretations that shed light on the instability mechanisms of the background flow (Wolfe and Samelson, 2006).

2.3. Singular vectors

Singular vectors optimize the growth of perturbations in a specified norm over a specified optimization interval $\tau = t_2 - t_1$. It is straightforward to show that the initial singular vectors $\boldsymbol{\xi}_{0,j}(t_1, t_2)$, initialized and optimized at times t_1 and t_2, respectively, are the eigenvectors of $\mathcal{L}(t_2, t_1)^*\mathcal{L}(t_2, t_1)$, where $\mathcal{L}(t_2, t_1)^*$ is the adjoint of $\mathcal{L}(t_2, t_1)$, defined by the identity $\langle \boldsymbol{v}, \mathcal{L}\boldsymbol{w}\rangle = \langle \mathcal{L}^*\boldsymbol{v}, \boldsymbol{w}\rangle$. The singular vectors can be evolved to any time t by application of the propagator. We will use the notation

$$\boldsymbol{\xi}_j(t; t_1, t_2) \equiv \mathcal{L}(t, t_1)\boldsymbol{\xi}_{0,j}(t_1, t_2), \tag{6}$$

to denote the singular vector with initialization and optimization times t_1 and t_2, respectively, which has been evolved to time t. The final singular vectors (often referred to as 'evolved' singular vectors) are simply $\boldsymbol{\xi}_j(t_2; t_1, t_2)$. They may also be obtained as the eigenvectors of $\mathcal{L}(t_2, t_1)\mathcal{L}(t_2, t_1)^*$.

If the inner product $\langle \cdot, \cdot \rangle$ is characterized by the matrix $\mathbf{N}$ such that

$$\langle \boldsymbol{v}, \boldsymbol{w}\rangle = \boldsymbol{v}^{\mathrm{T}}\mathbf{N}\boldsymbol{w}, \tag{7}$$

then

$$\mathbf{N}\mathcal{L}(t_2, t_1)^* = \mathcal{L}(t_2, t_1)^{\mathrm{T}}\mathbf{N}. \tag{8}$$

If the initial and final time norms are the same, the singular vectors and their amplification factors (the singular values) σ_j satisfy the generalized eigenvalue problem

$$\mathcal{L}(t_2, t_1)^{\mathrm{T}}\mathbf{N}\mathcal{L}(t_2, t_1)\boldsymbol{\xi}_j(t_1; t_1, t_2) = \sigma_j^2\mathbf{N}\boldsymbol{\xi}_j(t_1; t_1, t_2), \tag{9}$$

The eigenvalue problem (9) may be solved directly for systems where the range of singular value magnitudes is not too great. Otherwise, a more robust method is singular value decomposition, which allows square matrix $\mathbf{B}$ to be written as

$$\mathbf{B} = \mathbf{U}\mathbf{S}\mathbf{V}^{\mathrm{T}}, \tag{10}$$

where $\mathbf{U}$ and $\mathbf{V}$ are orthogonal matrices and $\mathbf{S}$ is diagonal (see, e.g. Golub and Van Loan, 1996). If eq. (10) is left-multiplied by $\mathbf{B}^{\mathrm{T}}$, singular value decomposition of $\mathbf{B}$ is seen to be equivalent to eigen-decomposition of $\mathbf{B}^{\mathrm{T}}\,\mathbf{B}$, since

$$\mathbf{B}^{\mathrm{T}}\mathbf{B} = \mathbf{V}\mathbf{S}\mathbf{U}^{\mathrm{T}}\mathbf{U}\mathbf{S}\mathbf{V}^{\mathrm{T}} = \mathbf{V}\mathbf{S}^2\mathbf{V}^{\mathrm{T}}. \tag{11}$$

Thus, eq. (11) will be equivalent to eq. (9) if

$$\mathbf{B} = \mathbf{N}^{1/2}\mathcal{L}(t_2, t_1)\mathbf{N}^{-1/2}, \tag{12}$$

$$\boldsymbol{v}_j = N^{1/2}\boldsymbol{\xi}_j(t_1; t_1, t_2) \tag{13}$$

and

$$\mathbf{S}_{jj} = \sigma_j, \tag{14}$$

where $\boldsymbol{v}_j$ is the j^{th} column of $\mathbf{V}$. Similarly, right multiplication of eq. (10) by $\mathbf{B}^{\mathrm{T}}$ shows that

$$\boldsymbol{u}_j = \sigma_j^{-1}\mathbf{N}^{1/2}\boldsymbol{\xi}_j(t_2; t_1, t_2), \tag{15}$$

where $\boldsymbol{u}_j$ is the j^{th} column of $\mathbf{U}$. The singular vectors for the examples of Section 4 were calculated using the singular value decomposition method.

2.4. *Lyapunov vectors: generalized normal modes*

The analysis of linear disturbances to flows with arbitrary time-dependence would be greatly facilitated by an appropriate generalization of normal modes. A suitable generalization of normal modes would have many potential applications, such as the diagnosis of the physical mechanisms responsible for instability and the maintenance of unsteady flow, as well as the discrimination between transient modal disturbance growth and non-modal growth mechanisms. A proper generalization of normal modes should characterize the asymptotic stability of linear disturbances to the flow, be norm-independent (and thus an intrinsic property of the trajectory), invariant under the linearized dynamics and reduce to traditional normal modes in the appropriate limits. The invariance under the linearized flow means that the n^{th} mode at time t_1 is transformed into the n^{th} mode at time t_2 by the linearized dynamics. Thus, as in standard normal mode theory for steady flows, all of the stability information is encoded in a fixed number of modes, which, in principle, need only be computed once. We argue in this section that Lyapunov vectors, appropriately defined, are the proper (though not necessarily the only) generalization of normal modes to aperiodic flows. First, however, we review the pertinent definitions and properties of Lyapunov exponents and Lyapunov vectors.

Lyapunov exponents characterize the asymptotic evolution of linear disturbances to bounded trajectories of arbitrary time dependence. The Lyapunov exponents $\lambda^{\pm}$ can be shown to be the logarithms of the eigenvalues of the matrices

$$\mathbf{S}_{\pm}(t_1) = \lim_{t_2\to\pm\infty}\left[\mathcal{L}(t_2, t_1)^*\mathcal{L}(t_2, t_1)\right]^{1/2(t_2-t_1)}. \tag{16}$$

These matrices exists under fairly general conditions (primarily, that the nonlinear trajectory exists and is bounded as $t \to \pm\infty$) and their eigenvalues are independent of norm and the initial time t_1 for almost every choice of t_1 (Oseledec, 1968). Furthermore, the forward and backward Lyapunov spectra are identical except for a change in sign, hence $\lambda_i^- = -\lambda_i^+$. We can thus unambiguously refer to $\lambda_i \equiv \lambda_i^+$ as *the* i^{th} Lyapunov exponent. Note that the Lyapunov spectrum may be degenerate, so that the total number of distinct Lyapunov exponents M may be less than the dimension of the system N.

Lyapunov vectors are the physical structures associated with the Lyapunov exponents. A norm-independent set of Lyapunov vectors ϕ_i, such that ϕ_i grows at the rate $\pm\lambda_i$ as $t \to \pm\infty$, may defined using the following consequence of the Oseledec (1968) theorem: For almost every time t, every vector $\boldsymbol{y}$ in the tangent space $\mathcal{S}_1^+(t) = \mathbb{R}^N$ of the dynamical system (1) grows asymptotically at a rate given by the first Lyapunov exponent λ_1 as the system evolves forward in time, except those $\boldsymbol{y}$ belonging to a set $\mathcal{S}_2^+(t)$ of measure zero. Similarly, every vector $\boldsymbol{y} \in \mathcal{S}_2^+(t)$ asymptotically grows at the rate λ_2 except those $\boldsymbol{y}$ belonging to a set $\mathcal{S}_3^+(t)$ of measure zero relative to $\mathcal{S}_2^+(t)$. This argument may be applied recursively to obtain a set of nested subspaces

$$\mathcal{S}_M^+(t) \subset \mathcal{S}_{M-1}^+(t) \subset \cdots \subset \mathcal{S}_1^+(t) = \mathbb{R}^N \tag{17}$$

such than any vector $\boldsymbol{y} \in \mathcal{S}_i^+(t) \setminus \mathcal{S}_{i+1}^+(t)$ grows asymptotically at the rate $\hat{\lambda}_i$, where $\hat{\lambda}_i$ is the i^{th} *distinct* Lyapunov exponent and $M \le N$ is the number of distinct Lyapunov exponents (Eckmann and Ruelle, 1985). The dimension of the difference space $\mathcal{S}_i^+(t) \setminus \mathcal{S}_{i+1}^+(t)$ is equal to the multiplicity m_i of $\hat{\lambda}_i$.

A similar argument may be made as the system evolved backward in time to obtain a similar set of nested subspaces

$$\mathcal{S}_M^-(t) \subset \mathcal{S}_{M-1}^-(t) \subset \cdots \subset \mathcal{S}_1^-(t) = \mathbb{R}^N \tag{18}$$

such than any vector $\mathbf{y} \in \mathcal{S}_i^-(t) \setminus \mathcal{S}_{i+1}^-(t)$ grows at the exponential rate $-\hat{\lambda}_i$. The intersection space

$$\mathcal{T}_i(t) = \mathcal{S}_i^+(t) \cap \mathcal{S}_{M-i+1}^-(t) \tag{19}$$

is, in general, m_i-dimensional, where m_i is the multiplicity of the i^{th} Lyapunov exponent. If $m_i = 1$, then $\mathcal{T}_i$ may be identified as *the* Lyapunov vector ϕ_i since it grows asymptotically at the rates $\hat{\lambda}_i$ and $-\hat{\lambda}_i$ as the system evolved forward and backward, respectively, in time. If $m_i > 1$, then any m_i linearly independent vectors from $\mathcal{T}_i$ may be identified as Lyapunov vectors.

The ϕ_i defined in this manner are norm-independent and characterize the asymptotic stability of linear disturbances as the system evolves both forward and backward in time. Furthermore, the ϕ_i reduce to the Floquet vectors if the flow is time-periodic (Trevisan and Pancotti, 1998) and to the stationary normal modes if the flow is stationary. Finally, the ϕ_i are invariant under the linearized flow, in the sense that they may, in principle, be computed once and then determined for all time using the tangent linear propagator. The Lyapunov vectors ϕ_i are thus good candidates for aperiodic normal modes.

This norm-independent definition of the Lyapunov vectors ϕ_i has been given previously by several authors (e.g. Vastano and Moser, 1991; Legras and Vautard, 1996; Trevisan and Pancotti, 1998). Note that Legras and Vautard (1996) call the ϕ_i 'characteristic vectors.' Trevisan and Pancotti (1998) show how these Lyapunov vectors may be obtained from singular vectors in the three-dimensional Lorenz (1963) system. Their method may, *in principle*, be extended to arbitrary N-dimensional systems, but would require the knowledge of $N + 1$ singular vectors. In modern forecast and process models, N is very large and this method would be prohibitively expensive. In Section 3, we give an efficient method for constructing the leading n Lyapunov vectors using just $2n-1$ singular vectors.

It should be noted that other definitions of Lyapunov vectors, which may be more appropriate for certain applications, are possible. Some authors define Lyapunov vectors to be the eigenvectors $\boldsymbol{\xi}^+$ of $\mathbf{S}_+$, equivalent to initial singular vectors optimized in the distant future (Goldhirsch et al., 1987; Yoden and Nomura, 1993). Others define Lyapunov vectors to be the eigenvectors $\boldsymbol{\xi}^-$ of $\mathbf{S}_+$, equivalent to final singular vectors optimized in the distant past (Lorenz, 1965, 1984; Shimada and Nagashima, 1979). Legras and Vautard (1996) consider both and call the former 'forward' Lyapunov vectors and the latter 'backward' Lyapunov vectors. These definitions produce norm-dependent Lyapunov vectors since, while the eigenvalues of $\mathbf{S}_\pm$ are independent of norm, the eigenvectors are not (except for the first or the last eigenvector). Lyapunov vectors defined in this manner are typically intended for use in predictability studies for which all that is required is a set of vectors which spans the same subspace as the growing disturbances.

However, these norm-dependent definitions are unsatisfactory for candidate aperiodic normal modes for a number of reasons. First, neither of these definitions reduce, in general, to stationary normal modes or Floquet vectors for stationary or time-periodic flows. Furthermore, the Lyapunov vectors defined as the eigenvectors of $\mathbf{S}_+$ or $\mathbf{S}_-$ do not characterize asymptotic stability forward nor the backward in time since, while the eigenvector $\boldsymbol{\xi}_i^+$ grows asymptotically with the rate λ_i as $t \to \infty$, it does not, in general, decay with the rate $-\lambda_i$ as $t \to -\infty$. Finally, neither the forward nor the backward Lyapunov vectors are invariant under the linearized flow and must be recomputed at each time of interest.

Singular vectors and finite-time normal modes (FTNM), the eigenvalues of the arbitrary-time propagator $\mathcal{L}(t_2, t_1)$ (Frederiksen, 1997), may also be considered, in some sense, to be generalizations of normal modes, but neither have both the required properties of norm-independence and invariance under the linearized dynamics. Singular vectors, in particular, depend strongly on the choice of norm and optimization interval. FTNMs are free from norm dependence, but still depend crucially on the choice of t_1 and t_2. While FTNMs are equivalent to time-stationary normal modes for time-stationary flows, if the flow is T-periodic, FTNMs reduce to Floquet vectors only if $t_2 - t_1 = nT$, for some integer $n \neq 0$. If $t_2 - t_1 \neq nT$, the eigenvectors and eigenvalues of $\mathcal{L}(t_2, t_1)$ lose their significance (Trevisan and Pancotti, 1998). For aperiodic flows, there is no way to choose a 'correct' value of $t_2 - t_1$. Furthermore, both singular vectors and FTNMs characterize transient stability only and it is possible to construct asymptotically stable systems, which nevertheless have growing singular vectors or FTNMs. Singular vectors and FTNM are also inconvenient from a computational point of view, since they must be computed *de novo* for each time interval of interest. The Lyapunov vectors defined above, in principle, need to be calculated at one time only and are then defined for all past and future times through the tangent linear propagator.

2.5. *Connections between Lyapunov vectors and singular vectors*

It is apparent from the discussion in the previous section that Lyapunov vectors are closely related to singular vectors with long optimization intervals. In fact, for sufficiently long optimization intervals, singular vectors are orthogonalizations of the Lyapunov vectors (Trevisan and Pancotti, 1998). To see how this is so, fix a time t and consider evolved singular vectors initialized in the distant past ($t_1 \ll t$) and optimized at t, i.e. consider

$$\hat{\boldsymbol{\eta}}_j(t) \equiv \lim_{t_1 \to -\infty} \boldsymbol{\xi}_j(t; t_1, t). \tag{20}$$

These singular vectors will be referred to as the 'backward' singular vectors since they are equivalent to Legras and Vautard's 'backward' Lyapunov vectors. Since almost all linear disturbances rotate towards the leading Lyapunov vector, we must have $\hat{\boldsymbol{\eta}}_1(t) = \hat{p}_{11}\boldsymbol{\phi}_1(t)$, for some projection coefficient $\hat{p}_{11}$. The second singular vector $\hat{\boldsymbol{\eta}}_2(t)$ is constrained to be orthogonal (in the selected inner product) to $\hat{\boldsymbol{\eta}}_1(t)$ at time t and thus cannot asymptotically approach the leading Lyapunov vector. Instead, the growth of $\hat{\boldsymbol{\eta}}_2(t)$ is optimized if it lies in $\mathcal{S}_2^+(t)$, the space spanned by the first two Lyapunov vectors. Thus, we must have $\hat{\boldsymbol{\eta}}_2(t) = \hat{p}_{21}\boldsymbol{\phi}_1(t) + \hat{p}_{22}\boldsymbol{\phi}_2(t)$. Recursive application of this argument gives a representation of the asymptotic evolved singular vectors $\hat{\boldsymbol{\eta}}_j(t)$ in terms of the Lyapunov vectors

$$\hat{\boldsymbol{\eta}}_j(t) = \sum_{i=1}^{j} \hat{p}_{ji}\boldsymbol{\phi}_i(t). \tag{21}$$

A similar argument can be made to show that the initial conditions of singular vectors optimized in the distant future $\hat{\boldsymbol{\xi}}_j(t)$ (called 'forward' singular vectors because they are equivalent to Legras and Vautard's 'forward' Lyapunov vectors), where

$$\hat{\boldsymbol{\xi}}_j(t) \equiv \lim_{t_2 \to \infty} \boldsymbol{\xi}_j(t; t, t_2), \tag{22}$$

are also an orthogonalization of the Lyapunov vectors. In this case, the orthogonalization proceeds upward from the most rapidly decaying Lyapunov vector to obtain

$$\hat{\boldsymbol{\xi}}_j(t) = \sum_{i=j}^{N} \hat{q}_{ji}\boldsymbol{\phi}_i(t), \tag{23}$$

for some coefficients $\hat{q}_{ji}$.

The convergence of the singular vectors to their asymptotic forms is, in fact, exponential. That this is a consequence of asymptotic exponential time-dependence of the Lyapunov vectors is made clearer by writing the propagator in terms of the Lyapunov vectors. Let

$$\mathcal{L}(t_2, t_1) = \mathbf{F}(t_2)\mathbf{F}(t_1)^{-1} \tag{24}$$

for any t_1, t_2, where $\mathbf{F}$ is a matrix whose columns are the Lyapunov vectors, ordered by decreasing Lyapunov exponent. Since the Lyapunov vectors span the space of linear disturbances, the singular vectors may be written as a fixed sum of Lyapunov vectors,

$$\boldsymbol{\xi}_j(t;t_1,t_2) = \sum_{i=1}^{N} \phi_i(t) p_{ij}(t_1,t_2) = \mathbf{F}(t)\boldsymbol{p}(t_1,t_2). \tag{25}$$

The projection coefficients are a function of initialization and optimization time only. With eqs. (24) and (25), (9) becomes

$$\mathbf{F}(t_2)^{\mathrm{T}}\mathbf{N}\mathbf{F}(t_2)\boldsymbol{p}_j = \sigma_j^2 \mathbf{F}(t_1)^{\mathrm{T}}\mathbf{N}\mathbf{F}(t_1)\boldsymbol{p}_j. \tag{26}$$

For $\tau = t_2 - t_1 \gg 1$, the components of the LHS of eq. (26) grow like

$$\left[\mathbf{F}(t_2)^{\mathrm{T}}\mathbf{N}\mathbf{F}(t_2)\right]_{ij} \sim e^{(\lambda_i+\lambda_j)\tau}. \tag{27}$$

Thus, as $\tau \to \infty$, the LHS of (26) is given with exponential accuracy by a matrix whose only non-zero entry is the upper right corner. The resulting eigensystem has only one nontrivial solution, $\boldsymbol{p}_1$, whose components are $p_{1i} = 0$ except for $i = 1$. The rate of convergence to the asymptotic form is $\mu_1 = |\lambda_2 - \lambda_1|$. The remaining eigenvectors can be recovered by working in the subspace orthogonal to the first, in which the LHS of eq. (26) is again given with exponential accuracy by a matrix whose only non-zero entry is the upper right corner. The rate of convergence in this subspace is $|\lambda_3 - \lambda_2|$, but since the rate of convergence *into* this subspace is $|\lambda_2 - \lambda_1|$, the rate of convergence of $\boldsymbol{\xi}_2(t;t_1, t)$ to its asymptotic form $\hat{\boldsymbol{\eta}}_2(t)$ is

$$\mu_2 = \min\{|\lambda_3 - \lambda_2|, |\lambda_2 - \lambda_1|\}. \tag{28}$$

In general, the rate of convergence of $\boldsymbol{\xi}_j(t;t_1, t)$ to its asymptotic form $\hat{\boldsymbol{\eta}}_j(t)$ is

$$\mu_j = \min_{1\le i\le j} |\lambda_{i+1} - \lambda_i|. \tag{29}$$

In a similar manner, it can be shown that the the rate of convergence of $\boldsymbol{\xi}_j(t;t, t_2)$ to its asymptotic form $\hat{\boldsymbol{\xi}}_j(t)$ is

$$\sigma_j = \min_{j\le i\le N} |\lambda_i - \lambda_{i-1}|. \tag{30}$$

It should be noted that μ_j and σ_j only give lower bounds on the convergence rate. For example, if two Lyapunov vectors are orthogonal in a given norm, the convergence rate of the corresponding singular vectors in that norm may be faster than the estimates given by μ_j and σ_j. In practice, we find that a good approximation to the true convergence rate is

$$\mu_j = \begin{cases} |\lambda_2 - \lambda_1| & j = 1, \\ \min\left\{|\lambda_{j+1} - \lambda_j|, |\lambda_j - \lambda_{j-1}|\right\} & 1 < j < N, \\ |\lambda_N - \lambda_{N-1}| & j = N, \end{cases} \tag{31}$$

Note that there is no useful lower bound on the convergence rate of singular vectors corresponding to Lyapunov exponents with multiplicity greater than one. The existence of the matrices $\mathbf{S}_\pm$ guarantees that these singular vectors will eventually approach asymptotic forms, but the convergence rate may be slower than exponential.

3. The recovery of Lyapunov vectors from singular vectors

The 'forward' and 'backward' asymptotic singular vectors $\hat{\boldsymbol{\eta}}_j$ and $\hat{\boldsymbol{\xi}}_j$, respectively, furnish two different orthogonalizations of the same Lyapunov vectors. It is possible to use these two orthogonalizations to recover the Lyapunov vectors in a norm-independent manner.

Under fairly general conditions, for each time t, the asymptotic forward and backward singular vectors ($\hat{\boldsymbol{\xi}}_j(t)$ and $\hat{\boldsymbol{\eta}}_j(t)$, respectively) are orthonormal in the specified norm and span the space of the dynamical system. Thus, each $\phi_i(t)$ may be alternately written as a linear combination of the $\hat{\boldsymbol{\xi}}$'s or the $\hat{\boldsymbol{\eta}}$'s. This may be expressed compactly as

$$\mathbf{F} = \mathbf{A}\mathbf{X}, \tag{32}$$

$$\mathbf{F} = \mathbf{B}\mathbf{Y}, \tag{33}$$

where $\mathbf{F}$, $\mathbf{X}$ and $\mathbf{Y}$ are matrices whose columns are the ϕ's, $\hat{\boldsymbol{\xi}}$'s and $\hat{\boldsymbol{\eta}}$'s, respectively, and the components of the matrices $\mathbf{A}$ and $\mathbf{B}$ are

$$a_{ij} = \langle \phi_i, \hat{\boldsymbol{\xi}}_j \rangle,$$
$$b_{ij} = \langle \phi_i, \hat{\boldsymbol{\eta}}_j \rangle.$$

If we could determine either $\mathbf{A}$ or $\mathbf{B}$, we could determine $\mathbf{F}$ and, thus, the Lyapunov vectors.

The relationships (32) and (33) may be inverted to find

$$\mathbf{X} = \mathbf{A}^{-1}\mathbf{F}, \tag{34}$$

$$\mathbf{Y} = \mathbf{B}^{-1}\mathbf{F}. \tag{35}$$

Comparison of eqs. (34) and (35) with eqs. (21) and (23) shows that $\mathbf{A}^{-1}$ is an upper triangular matrix with components $\hat{q}_{ji}$ and $\mathbf{B}^{-1}$ is a lower triangular matrix with components $\hat{p}_{ji}$. It follows that $\mathbf{A}$ is upper triangular and $\mathbf{B}$ is lower triangular: $\langle \phi_i, \hat{\boldsymbol{\xi}}_j \rangle = 0$ for $i < j$ and $\langle \phi_i, \hat{\boldsymbol{\eta}}_j \rangle = 0$ for $i > j$. Thus, eq. (32) and (33) may be written as

$$\phi_n = \sum_{i=n}^{N} \langle \hat{\boldsymbol{\xi}}_i, \phi_n \rangle \hat{\boldsymbol{\xi}}_i, \tag{36}$$

$$\phi_n = \sum_{j=1}^{n} \langle \hat{\boldsymbol{\eta}}_j, \phi_n \rangle \hat{\boldsymbol{\eta}}_j, \tag{37}$$

where now the dependence of all the vectors on t has been suppressed.

Setting eq. (36) equal to eq. (37) gives

$$\sum_{j=1}^{n}\langle\hat{\boldsymbol{\eta}}_j,\phi_n\rangle\hat{\boldsymbol{\eta}}_j=\sum_{i=n}^{N}\langle\hat{\boldsymbol{\xi}}_i,\phi_n\rangle\hat{\boldsymbol{\xi}}_i$$

which, upon taking inner products alternately with $\hat{\boldsymbol{\xi}}_k$ and $\hat{\boldsymbol{\eta}}_k$, yields

$$\langle\hat{\boldsymbol{\xi}}_k,\phi_n\rangle=\sum_{j=1}^{n}\langle\hat{\boldsymbol{\eta}}_j,\phi_n\rangle\langle\hat{\boldsymbol{\xi}}_k,\hat{\boldsymbol{\eta}}_j\rangle\quad\text{for}\quad k\geq n, \tag{38}$$

$$\langle\hat{\boldsymbol{\eta}}_k,\phi_n\rangle=\sum_{i=n}^{N}\langle\hat{\boldsymbol{\xi}}_i,\phi_n\rangle\langle\hat{\boldsymbol{\eta}}_k,\hat{\boldsymbol{\xi}}_i\rangle\quad\text{for}\quad k\leq n. \tag{39}$$

Substitution of eq. (38) into eq. (37) to eliminate $\langle\hat{\boldsymbol{\xi}}_k,\phi_n\rangle$ yields the following linear system in $\langle\hat{\boldsymbol{\eta}}_k,\phi_n\rangle$:

$$\langle\hat{\boldsymbol{\eta}}_k,\phi_n\rangle=\sum_{j=1}^{n}\left[\sum_{i=n}^{N}\langle\hat{\boldsymbol{\eta}}_k,\hat{\boldsymbol{\xi}}_i\rangle\langle\hat{\boldsymbol{\xi}}_i,\hat{\boldsymbol{\eta}}_j\rangle\right]\langle\hat{\boldsymbol{\eta}}_j,\phi_n\rangle\quad k\leq n. \tag{40}$$

The solution to this system gives the expansion coefficients of the Lyapunov vectors in terms of the backward singular vectors, which, in turn, determines the Lyapunov vectors themselves. However, the solution of (40) for any n requires the knowledge of $N+1$ asymptotic singular vectors and the accuracy of the solution is limited by the accuracy of the singular vector with the slowest convergence rate. If the Lyapunov spectrum is degenerate, convergence of (40) is not assured for any finite optimization interval τ.

The bracketed term in (40) can be simplified and the convergence problem circumvented by noting that for any two complete orthonormal sets of vectors $\boldsymbol{e}_i$ and $\boldsymbol{f}_i$,

$$\sum_{k=1}^{N}\langle\boldsymbol{f}_i,\boldsymbol{e}_k\rangle\langle\boldsymbol{e}_k,\boldsymbol{f}_j\rangle=\delta_{ij}.$$

Thus,

$$\sum_{i=n}^{N}\langle\hat{\boldsymbol{\eta}}_k,\hat{\boldsymbol{\xi}}_i\rangle\langle\hat{\boldsymbol{\xi}}_i,\hat{\boldsymbol{\eta}}_j\rangle=\delta_{kj}-\sum_{i=1}^{n-1}\langle\hat{\boldsymbol{\eta}}_k,\hat{\boldsymbol{\xi}}_i\rangle\langle\hat{\boldsymbol{\xi}}_i,\hat{\boldsymbol{\eta}}_j\rangle$$

and therefore,

$$\sum_{j=1}^{n}\sum_{i=1}^{n-1}\langle\hat{\boldsymbol{\eta}}_k,\hat{\boldsymbol{\xi}}_i\rangle\langle\hat{\boldsymbol{\xi}}_i,\hat{\boldsymbol{\eta}}_j\rangle\langle\hat{\boldsymbol{\eta}}_j,\phi_n\rangle=0\quad k\leq n. \tag{41}$$

That this is indeed a simplification becomes apparent when it is noted that eq. (41) involves only the first $n-1$ forward and n backward asymptotic singular vectors.

Eqs. (40) and (41) can be cast into a more familiar form by defining

$$y_k^{(n)}=\langle\hat{\boldsymbol{\eta}}_k,\phi_n\rangle\quad k=1,2,\ldots,n, \tag{42}$$

$$D_{kj}^{(n)}=\sum_{i=1}^{n-1}\langle\hat{\boldsymbol{\eta}}_k,\hat{\boldsymbol{\xi}}_i\rangle\langle\hat{\boldsymbol{\xi}}_i,\hat{\boldsymbol{\eta}}_j\rangle\quad k,j\leq n. \tag{43}$$

Then eq. (41) takes the form

$$\mathbf{D}^{(n)}\boldsymbol{y}^{(n)}=0, \tag{44}$$

and the desired expansion coefficients $\boldsymbol{y}^{(n)}$ are seen to be the null vector of $\mathbf{D}^{(n)}$. The problem (44) can thus be solved to obtain the n leading Lyapunov vectors from just the first $n-1$ forward and n backward singular vectors. In contrast, the expansion (40) requires the knowledge of $N+1$ singular vectors. In many ensemble forecasting examples, $2n-1\ll N+1$.

A similar method for recovering the last n Lyapunov vectors from the last n forward and $n-1$ backward singular vectors may be obtained by substituting (37) into (38) to eliminate $\langle\hat{\boldsymbol{\eta}}_k,\phi_n\rangle$ and proceeding as above. The trailing Lyapunov vectors are then the null vectors of

$$\mathbf{C}^{(n)}\boldsymbol{x}^{(n)}=0, \tag{45}$$

where

$$x_k^{(n)}=\langle\hat{\boldsymbol{\xi}}_{k+n-1},\phi_n\rangle\quad k=1,2,\ldots,N-n+1, \tag{46}$$

and

$$C_{ki}^{(n)}=\sum_{j=n+1}^{N}\langle\hat{\boldsymbol{\xi}}_{k+n-1},\hat{\boldsymbol{\eta}}_j\rangle\langle\hat{\boldsymbol{\eta}}_j,\hat{\boldsymbol{\xi}}_{i+n-1}\rangle\quad k,i\leq N-n+1. \tag{47}$$

The uniqueness of the recovered Lyapunov vectors [the solution to eqs. (44) and (45)] follows from the uniqueness of the representations (36) and (37) which, in turn, follows from the completeness of the asymptotic singular vectors and assumed uniqueness of the Lyapunov vectors in question. As discussed in Sections 2.4 and 2.5, the Lyapunov vectors associated with Lyapunov exponents with multiplicity $m_i>1$ are not uniquely defined and the above method may produce unpredictable results when applied to these Lyapunov vectors. The extension of these results to the case of degenerate Lyapunov vectors is a subject of future work.

Note that the $\hat{\boldsymbol{\eta}}_j$ could be replaced with *any* orthogonal set of linear disturbances initialized sufficiently far in the past, although the singular vectors are, by definition, optimal. The same is not true for the $\hat{\boldsymbol{\xi}}_j$ since the efficiency of this algorithm depends crucially on the fact that the $\hat{\boldsymbol{\xi}}_j$ are initial conditions, which optimize disturbance growth in the future. This is necessary to ensure that the $\hat{\boldsymbol{\xi}}_j$ are a proper orthogonalization of the Lyapunov vectors (i.e. one that proceeds upwards from the most rapidly decaying Lyapunov vector). Replacement of the $\hat{\boldsymbol{\xi}}_j$ with a different, non-optimal, set of linear disturbances would require using a complete set of linear disturbances initialized in the distant future and integrated backward to t in order to obtain the correct orthogonalization. Evolving such a complete set of linear disturbances would negate the efficiency of this method.

4. Numerical examples

4.1. Lorenz model

The Lorenz model is perhaps the simplest nontrivial system with which to demonstrate the principles discussed in Section 2.5 and the algorithm presented in Section 3. The development and characteristics of this model are well studied, and the reader is referred to the extensive literature (e.g. Sparrow, 1982) regarding this model for further details. Furthermore, since the linear disturbance dynamics of this model have been discussed in detail by other authors (e.g. Legras and Vautard, 1996; Trevisan and Legnani, 1995; Trevisan and Pancotti, 1998), the present treatment of the Lorenz model will be brief.

We use the standard parameter values $\sigma = 10$, $\rho = 28$, and $\beta = 8/3$, for which the model possesses a strange attractor with Lyapunov exponents

$$\lambda_1 = 0.91 \pm 0.01,$$

$$\lambda_2 = 0,$$

$$\lambda_3 = -14.58 \pm 0.01.$$

That λ_2 is exactly zero is a consequence of the fact that the model equations do not explicitly depend on time. Furthermore, it can be shown that, if the Lyapunov vectors are defined in terms of intersecting forward and backward subspaces (as in Section 2.4), the second Lyapunov vector ϕ_2 is proportional to the time derivative (i.e. the tangent vector) of the nonlinear trajectory. Since ϕ_2 is the only Lyapunov vector that requires a non-trivial application of the method described in Section 3 for three-dimensional systems, this result will prove to be a useful check of the calculation.

The propagator $\mathcal{L}$ was obtained on a fine temporal grid ($\Delta t = 0.02$) by direct integration of the tangent linearization of the Lorenz equations about a nonlinear, aperiodic trajectory encompassing 8 time units. The singular vectors in the identity norm were then calculated by singular value decomposition of $\mathcal{L}$. The asymptotic forms of the singular vectors were obtained by, at each point in the temporal grid, systematically increasing the optimization interval τ until the singular vectors were constant to within a specified tolerance (here, 10^{-6}). As discussed in Section 2.5, the convergence of the singular vectors to their asymptotic forms was expected to be asymptotically exponential. According to the estimate (31), the average convergence rate of the first and second singular vectors was expected to be $\lambda_1 - \lambda_2 = \lambda_1$ while the expected average convergence rate of the third singular vector was $\lambda_2 - \lambda_3 = -\lambda_3$. The observed numerical convergence rates (Fig. 1) matched these expectations quite well.

The Lyapunov vectors ϕ_j were calculated from the singular vectors using the method described in Section 3. The second Lyapunov vector ϕ_2 was found to subtend an angle of only $0.02^\circ \pm 0.01^\circ$ with the tangent vector of the trajectory. The numerically determined second Lyapunov vector was thus nearly collinear with the tangent vector of the trajectory, which indicated that the algorithm was operating correctly.

The local Lyapunov exponents (LLEs),

$$\mathrm{LLE}_j(t) = \frac{1}{\|\phi_j(t)\|}\frac{d}{dt}\|\phi_j(t)\|, \tag{48}$$

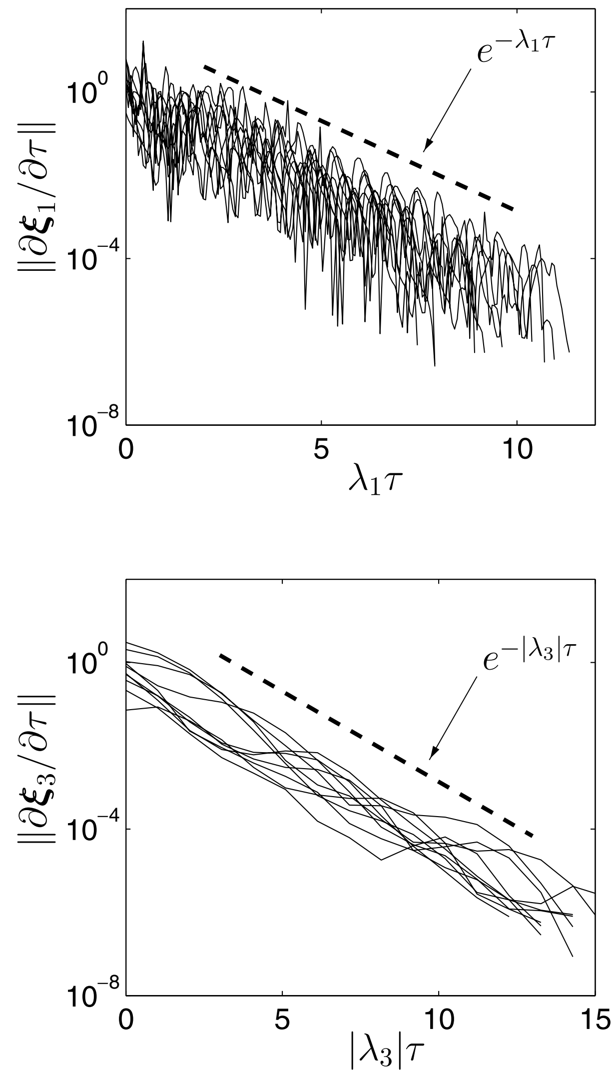

Fig. 1. Norm of the derivative of the first (upper panel) and last (lower panel) forward singular vectors with respect to optimization interval τ as a function of τ for 10 different initialization times scattered throughout the attractor. The dotted lines give the expected convergence rates predicted by the Lyapunov exponents of the Lorenz model.

of the first two Lyapunov vectors are of comparable magnitude and show marked oscillations in phase with the growth and decay of the underlying trajectory (Fig. 2b). The LLE of the last, rapidly decaying, Lyapunov vector shows similar oscillations roughly 180° out of phase with the leading two Lyapunov vectors, indicating that the growth phase of the underlying trajectory is favourable for enhanced transient decay as well as growth. Note that the first two Lyapunov vectors exhibit many periods of so-called 'super-Lyapunov' growth, that is, their local growth rates are larger than the leading Lyapunov exponent. While super-Lyapunov growth is sometimes taken as evidence of non-modal dynamics, the dynamics here are modal by definition. Thus, the normal modes themselves are capable of transient growth exceeding that of the first Lyapunov exponent; only their long-time average growth rate is bounded by the Lyapunov exponents. The relationship between super-Lyapunov growth and modal dynamics is discussed in detail by Trevisan and Pancotti (1998).

The projections of the Lyapunov vectors onto each other also oscillate with the nonlinear trajectory (Fig. 2c). The first two Lyapunov vectors are nearly collinear during the trajectory maxima and nearly orthogonal during the trajectory minima. The projections of ϕ_1 and ϕ_2 onto the third, decaying, Lyapunov vector ϕ_3 are of similar magnitude and are generally smaller than their projections onto each other. The time evolution of the projections are very similar to that found by Trevisan and Pancotti (1998), although the detailed behaviour is different because those authors focused on a time-periodic trajectory of the Lorenz model while the current trajectory is aperiodic.

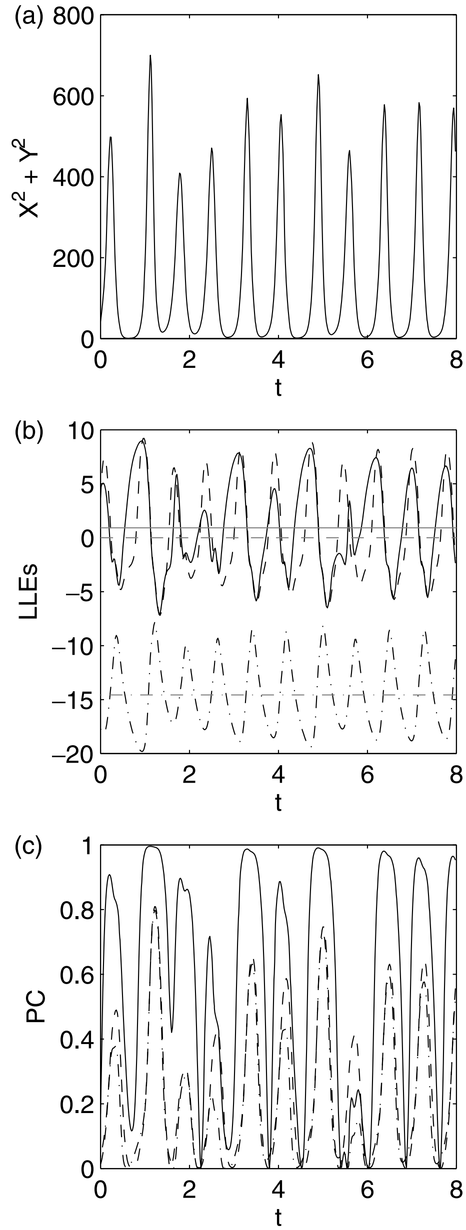

Fig. 2. (a) Background flow amplitude as measured by $X^2 + Y^2$, (b) local Lyapunov exponents (LLEs) of ϕ_1 (solid), ϕ_2 (dashed), ϕ_3 (dash-dot) and (c) pattern correlation between ϕ_1 and ϕ_2 (solid), ϕ_2 and ϕ_3 (dashed) and ϕ_3 and ϕ_1 (dash-dot) as a function of time for the Lorenz model. The horizontal gray lines in (b) give the Lyapunov exponent associated with each Lyapunov vector. Compare (c) to Trevisan and Pancotti (1998), Fig. 4.

4.2. *Weakly nonlinear Phillips model*

The weakly non linear Phillips model of the baroclinic instability (Pedlosky, 1971) can be formally considered to be an extension of the Lorenz model (Pedlosky and Frenzen, 1980). It has the advantage of being a consistent asymptotic limit of a geophysical process, whereas the Lorenz equations result from an ad hoc truncation of the equations of motion. This enables us to interpret the convergence time-scale of the singular vectors in terms of a physically relevant time-scale.

The weakly non-linear model is described in detail in Pedlosky (1987, section 7.16). It takes the form of a system of non-linear ordinary differential equations for the amplitude A (proportional to the barotropic streamfunction) and inter-layer phase shift B (proportional to the baroclinic streamfunction) of a baroclinic wave. The presence of the wave induces a change in the zonal mean flow which is described by the mean flow corrections V_j. While there are, in principle, an infinite number of mean flow correction terms, in practice, only a finite number J are retained. We use $J = 6$, the same value used by Samelson (2001a,b); the system considered here is thus 8-dimensional. The behaviour of the model is controlled by three parameters: the zonal and meridional wavenumbers (k, m) of the fundamental wave and the dissipation parameter γ. For $(k, m) = (\pi, 1)$ and $\gamma = 0.1315$, the model undergoes a baroclinic wave-mean oscillation of chaotically vacillating amplitude with mean period $T_p \approx 24.4$ (for details, see Samelson, 2001a,b).

Direct calculation of the Lyapunov exponents λ_i, using standard methods (e.g. Bennetin et al., 1980), yields

$$
\begin{aligned}
\lambda_1 &= 0.0178 \pm 0.0002,\\
\lambda_2 &= 0,\\
\lambda_3 &= -0.0797 \pm 0.0001,\\
\lambda_8 &= -0.2877 \pm 0.0002,
\end{aligned}
$$

while $\lambda_i \approx -\gamma$ for $i = 4, 5, 6, 7$. The differences between the exponents λ_4 through λ_7 are thus small and, by the convergence rate estimate (31), the corresponding singular vectors can be expected to converge very slowly. The other singular vectors show a range of expected convergence times, from about a quarter

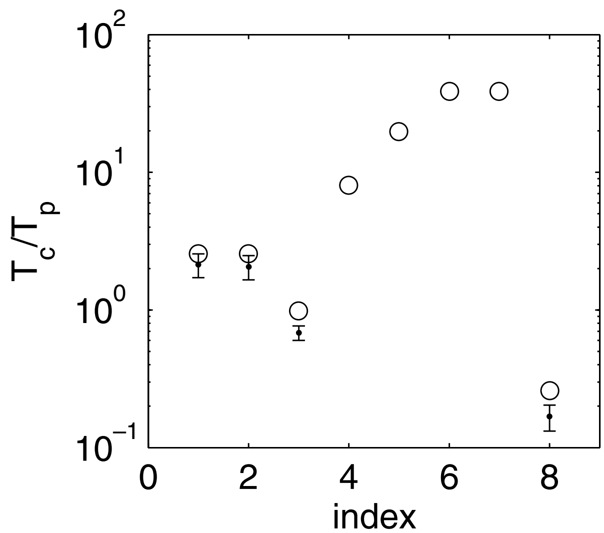

Fig. 3. Singular vector convergence e-folding time T_c relative to the mean period of the baroclinic wave-mean oscillation T_p for the weakly nonlinear Phillips model. Circles give the expected convergence time based on the Lyapunov exponents, dots give the average measured convergence time (based on a fit to an exponential) for ten initial randomly chosen initial conditions, and the error bars give the standard deviation. The asymptotic forms were not calculated for singular vectors 4–7.

period for $\hat{\xi}_8$ to more than $2.5T_p$ for $\hat{\xi}_1$ and $\hat{\xi}_2$. The expected convergence time for singular vectors $\hat{\xi}_4$ through $\hat{\xi}_7$ is greater than $10T_p$ (Fig. 3), and we therefore omit calculating $\hat{\xi}_4$ through $\hat{\xi}_7$.

The asymptotic singular vectors $\hat{\xi}_1$, $\hat{\xi}_2$, $\hat{\xi}_3$ and $\hat{\xi}_8$ in the identity norm were calculated on a coarse temporal grid ($\Delta t = 5$) using the same method as in Section 4.1, with a convergence tolerance of 10^{-4}. The singular vectors converged to their asymptotic forms slightly faster than predicted (Fig. 3).

The first three Lyapunov vectors were recovered from the asymptotic singular vector on the coarse grid using the method of Section 3. Integration of the tangent linear equations using the recovered Lyapunov vectors as initial conditions was used to determine the Lyapunov vectors on a refined temporal grid ($\Delta t = 0.1$). The advantage of this method was two-fold: first, it allowed the transient growth and decay of the Lyapunov vectors to be determined (the method of Section 3 cannot determine the amplitude of the Lyapunov vectors); second, integration of the tangent linear equations was much more efficient than calculating asymptotic singular vectors on a fine temporal grid. Since the Lyapunov vectors were not determined to perfect accuracy, the tangent linear integration could be performed for only a finite time before all of the vectors began to rotate toward the leading Lyapunov vector. It was found, through trail-and-error, that restarting the tangent linear integration every $\Delta t = 5$ gave a good trade-off between accuracy and computational effort. The resulting Lyapunov vectors grew or decayed at the correct rate, as given by the Lyapunov exponents (Fig. 4). Furthermore, the second Lyapunov vector ϕ_2 tracked the transient growth and decay of the tangent to the background trajectory quite well (grey dash-dotted line in Fig. 4). It should be noted that the decaying Lyapunov vector ϕ_3 could not have been obtained by long forward or backward integration (which gives only the first or last Lyapunov vectors, respectively), nor could it have been obtained using the straightforward extension of the methods presented in Legras and Vautard (1996) and Trevisan and Pancotti (1998) due to the unavailability of the asymptotic singular vectors $\hat{\xi}_4$ through $\hat{\xi}_7$.

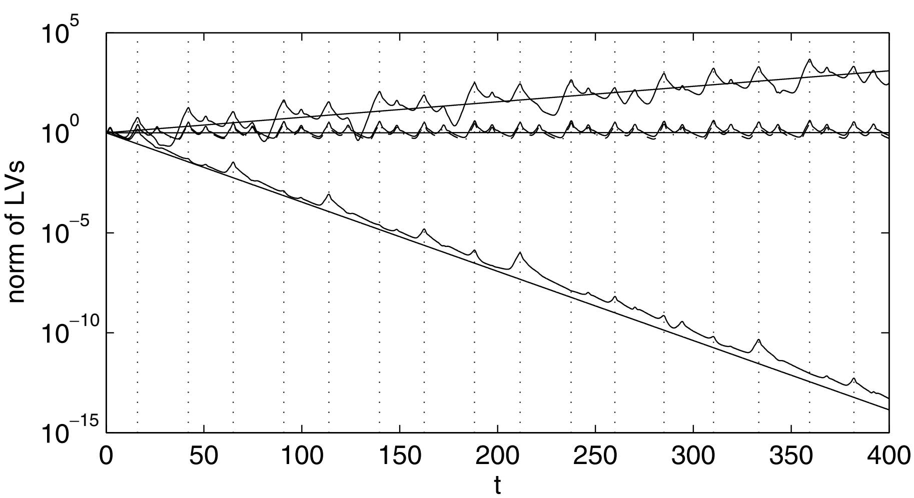

Fig. 4. Norm of the first three Lyapunov vectors (solid) and the tangent to the background trajectory (dash-dot, grey) as a function of time. The expected exponential growth calculated from the Lyapunov exponents is shown for reference (dashed). Vertical dotted lines give the location of the Poincaré section $B = \gamma A$, $A > 0$.

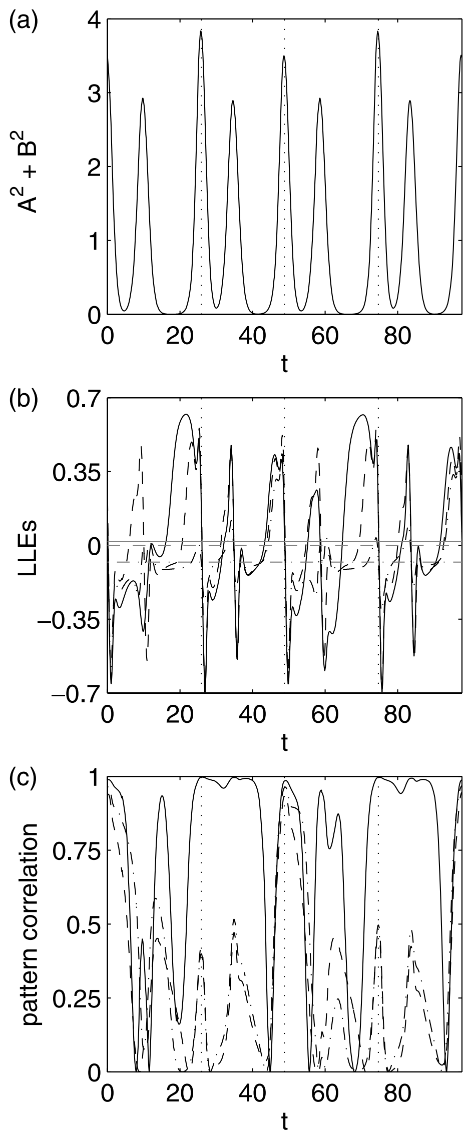

Fig. 5. (a) Background flow 'energy' as measured by $A^2 + B^2$, (b) local Lyapunov exponents (LLEs) of ϕ_1 (solid), ϕ_2 (dashed), ϕ_3 (dash-dot) and (c) pattern correlation between ϕ_1 and ϕ_2 (solid), ϕ_2 and ϕ_3 (dashed) and ϕ_3 and ϕ_1 (dash-dot) as a function of time for the same time interval as Fig. 4. The horizontal grey lines in (b) give the Lyapunov exponent associated with each Lyapunov vector. Vertical dotted lines give the location of the Poincaré section $B = \gamma A$, $A > 0$.

The leading three Lyapunov vectors give an interesting picture of the dynamics of linear disturbances to the aperiodic trajectory. ϕ_2, since it is proportional to the time-derivative of the background trajectory, grows and decays in phase with the growth and decay phases of the background trajectory (Fig. 5b) and directly reflects the dynamics of the aperiodic trajectory itself. ϕ_1 and ϕ_3 have similar local growth rates and grow and decay roughly in phase with ϕ_2; there are, however, important differences. ϕ_1 goes through periods of high and low activity, which are associated with times when the background trajectory achieves relatively high or low amplitude, respectively, on the Poincaré section $B = \gamma A$, $A > 0$ (compare Fig. 5a with Fig. 5b). In contrast, ϕ_3 is most active when ϕ_1 is least active.

The projections of the Lyapunov vectors onto each other are of interest because systems with highly non-orthogonal Lyapunov vectors are capable of rapid transient growth due to the interference of the Lyapunov vectors (Farrell and Ioannou, 1996). Following a high-activity period, ϕ_1 spends an extended period of time nearly collinear with ϕ_2 (Fig. 5c). Thus, while disturbances with strong projections onto ϕ_1 will grow during a high-activity period simply because ϕ_1 is growing, disturbances made after a high-activity period may still grow through interference of ϕ_1 and ϕ_2, even when all of the LLEs are negative. The temporal evolution of the projection of ϕ_1 onto ϕ_2 is more structured following a low-activity period and contains several periods of orthogonality (Fig. 5c). The projections of both ϕ_1 and ϕ_2 onto ϕ_3 are of similar magnitude and generally smaller than their projections onto each other. However, all three Lyapunov vectors are nearly orthogonal approximately 5 time units ahead of a low-activity Poincaré section but rotate to become nearly collinear on the low-activity Poincaré sections ($t \approx 0$, 50, 100).

The above observations were derived from a short segment of an aperiodic trajectory. In order to test if they held more generally, Lyapunov vectors where calculated from a long trajectory ($T = 20\,000$) at equal intervals of $\Delta t = 5$. Four thousand points were sufficient to give good coverage of the attractor, which may be conveniently visualized in the $(A, B - \gamma A)$ plane (Fig. 6). In this representation, the wave-mean oscillation takes the form of a 'dog-bone' shaped structure. The sense of motion on the attractor is clockwise. The amplitude vacillation is strongest on the right-hand side of the dog-bone, where the trajectories show the most spread. Most of the following discussion will focus on this region of the attractor.

The Lyapunov vector ϕ_2, which is proportional to the time-derivative of the aperiodic trajectory, grows and decays as the background trajectory grows and decays and shows little variation transverse to the attractor (Fig. 6b). The growth of ϕ_1 starts earlier than that of ϕ_2 and is slightly stronger on the 'outside' edge of the attractor (Fig. 6a); thus, the high-activity phases of ϕ_1 coincide with the high-amplitude phases of the background trajectory. In contrast, growth of ϕ_3 is weaker and starts later than the growth of ϕ_2 (Fig. 6c). Both growth and decay of ϕ_3 are strongest on the inside edge of the attractor.

The behaviour of the projections between the Lyapunov vectors is similar, in general, to that deduced from the short aperiodic segment. The first two Lyapunov vectors are nearly collinear at most points on the attractor, with a brief episode of near-orthogonality near the beginning of the right-hand growth cycle (Fig. 6d). There is an additional region of near-orthogonality near the beginning of the left-hand growth cycle, but this region is

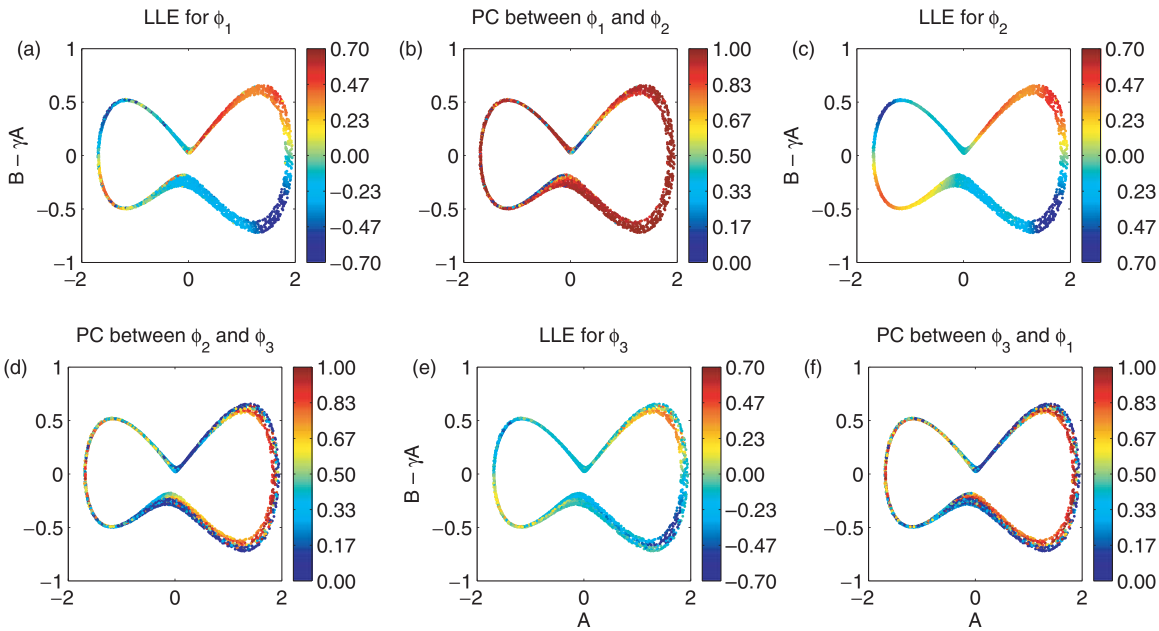

Fig. 6. Scatter plots of A vs. $B - \gamma A$ at 4000 equally spaced times. Colours give the local Lyapunov exponent (upper panels) and pattern correlations (lower panels) at each time.

localized on the inward-facing part of the attractor. Thus, a period of near-orthogonality follows a low-amplitude phase, but not a high amplitude phase. The projections of both ϕ_1 and ϕ_2 onto ϕ_3 are again of similar magnitude and generally smaller than their projections onto each other, with near-orthogonality prevalent during high-amplitude phases and near-collinearity prevalent during low-amplitude phases.

5. DISCUSSION

The method described in this paper allows the first n Lyapunov vectors to be constructed in a norm-independent manner from the first $n - 1$ asymptotic forward and first n backward singular vectors. The method has been demonstrated here for two idealized geophysical examples and are found to provide a useful picture of the phase-space dynamics of linear disturbances.

Several studies have successfully used the leading Lyapunov vector to understand the physics of aperiodic flow and the maintenance of chaotic behaviour (e.g. Vastano and Moser, 1991; Vannitsem and Nicolis, 1997; Wei and Frederiksen, 2004). Even though Lyapunov exponents and thus Lyapunov vectors are defined asymptotically, Lyapunov vectors can be useful for understanding short-time dynamics, such as transient error growth (Trevisan and Pancotti, 1998). Next-to-leading and even decaying Floquet vectors capture interesting dynamical processes in time-periodic systems (Wolfe and Samelson, 2006). As demonstrated in Section 4.2, non-leading, but norm-independent, Lyapunov vectors are similarly useful in the analysis of aperiodic flow. The algorithm presented here allows these Lyapunov vectors to be obtained in an efficient manner.

Demonstration of the method in a strongly nonlinear, high-dimensional baroclinic flow (Samelson and Wolfe, 2003; Wolfe and Samelson, 2006) is in progress and will be reported elsewhere. It is interesting to consider whether a version of this method might be obtained to estimate atmospheric Lyapunov vectors from operational forecast models, for which forward singular vectors are routinely calculated (e.g. Buizza and Palmer, 1995). It should be noted that the ensemble initialization cycle usually includes an analysis phase which adjusts the nonlinear trajectory in a manner that may be inconsistent with the dynamical equations, and the effect of this on the convergence of the singular vectors is not yet known.

A practical obstacle to the extraction of atmospheric Lyapunov vectors from operational singular vectors will be the limited degree to which operational singular vectors can be considered asymptotic, as the simple baroclinic wave example suggests that the required optimization times may span more than one baroclinic life cycle. However, the method may still yield interesting approximate results and future work may lead to useful extensions and refinements of the approach.

6. Acknowledgments

The authors gratefully acknowledge the Office Naval Research, Grants N00014-98-1-0813 and N00014-06-1-0369, Code 322 OM, for support of this work. The suggestions of two anonymous referees substantially improved this text.

References

Bennetin, G., Galgani, L., Giorgilli, A. and Strelcyn, J.-M. 1980. Lyapunov characteristic exponents for smooth dynamical systems and for Hamiltonian systems: A method for computing all of them. *Meccanica* **15**, 9–21.

Buizza, R. and Palmer, T. 1995. The singular vector structure of the atmospheric general circulation. *J. Atmos. Sci.* **52**, 1434–1456.

Buizza, R., Houtekamer, P. L., Toth, Z., Pellerin, G., Wei, M. and co-authors. 2005. A comparison of the ECMWF, MSC and NCEP global ensemble prediction systems. *Mon. Wea. Rev.* **133**, 1076–1097.

Coddington, E. A. and Levinson, N. 1955. *Theory of Ordinary Differential Equations*. McGraw Hill, New York.

Drazin, P. G. and Reid, W. H. 2004. *Hydrodynamical Stability*. 2nd edition, Cambridge University Press, Cambridge, UK.

Eckmann, J.-P. and Ruelle, D. 1985. Ergodic theory of chaos and strange attractors. *Rev. Mod. Phys.* **57**, 617–656.

Farrell, B. F. 1989. Optimal excitation of baroclinic waves. *J. Atmos. Sci.* **46**, 1193–1206.

Farrell, B. F. and Ioannou, P. J. 1996. Generalized stability theory part I: Autonomous operators. *J. Atmos. Sci.* **53**, 2025–2040.

Frederiksen, J. S. 1997. Adjoint sensitivity and finite-time normal mode disturbances during blocking. *J. Atmos. Sci.* **54**, 1144–1165.

Goldhirsch, I., Sulem, P. L. and Orszag, A. 1987. Stability and lyapunov stability of dynamical systems: A differential approach and a numerical method. *Phyisca D* **27**, 311–337.

Golub, G. H. and Van Loan, C. F. 1996. *Matrix Computations* 3rd edition The Johns Hopkins University Press Ltd, London.

Legras, B. and Vautard, R. 1996. A guide to Liapunov vectors. In: *Predictability, Volume I*. European Centre for Medium-Range Weather Forecasts, 143–156.

Lorenz, E. N. 1963. Deterministic non-periodic flow. *J. Atmos. Sci.* **20**, 130–141.

Lorenz, E. N. 1965. A study of the predictability of a 28-variable atmospheric model. *Tellus* **17**, 321–333.

Lorenz, E. N. 1984. The local structure of a chaotic attractor in four dimensions. *Physica D* **13**, 90–104.

Oseledec, V. 1968. A multiplicative ergodic theorem. Lyapunov characteristic numbers for dynamical systems. *Trans. Moscow Math. Soc.* **19**, 179–210.

Pedlosky, J. 1971. Finite-amplitude baroclinic waves with small dissipation. *J. Phys. Oceanogr.* **28**, 587–597.

Pedlosky, J. 1987. *Geophysical Fluid Dynamics*. 2nd edition. Springer.

Pedlosky, J. and Frenzen, C. 1980. Chaotic and periodic behavior of finite-amplitude baroclinic waves. *J. Atmos. Sci.* **37**, 1177–1196. New York.

Samelson, R. M. 2001a. Lyapunov, floquet, and singular vectors for baroclinic waves. *Nonlinear Processes Geophys.* **8**, 439–448.

Samelson, R. M. 2001b. Periodic orbits and disturbance growth for baroclinic waves. *J. Atmos. Sci.* **58**, 436–450.

Samelson, R. M. and Wolfe, C. L. 2003. A nonlinear baroclinic wave-mean oscillation with multiple normal mode instabilities. *J. Atmos. Sci.* **60**, 1186–1199.

Shimada, I. and Nagashima, T. 1979. A numerical approach to the ergodic problem of dissipative dynamical systems. *Prog. Theor. Phys.* **61**, 1605–1616.

Sparrow, C. 1982. *The Lorenz Equations: Bifurcations, Chaos, and Strange Attractors*. Springer-Verlag, New York.

Trevisan, A. and Legnani, R. 1995. Transient error growth and local predictability: A study of the Lorenz system. *Tellus* **47A**, 103–117.

Trevisan, A. and Pancotti, F. 1998. Periodic orbits, Lyapunov vectors, and singular vectors in the Lorenz system. *J. Atmos. Sci.* **55**, 390–398.

Vannitsem, S. and Nicolis, C. 1997. Lyapunov vectors and error growth patterns in a T21L3 quasigeostrophic model. *J. Atmos. Sci.* **54**, 357–361.

Vastano, J. A. and Moser, R. D. 1991. Short-time Lyapunov exponent analysis and the transition to chaos in Taylor-Couette flow. *J. Fluid Mech.* **233**, 83–118.

Wei, M. and Frederiksen, J. S. 2004. Error growth and dynamical vectors during southern hemisphere blocking. *Nonlinear Processes Geophys.* **11**, 99–118.

Wolfe, C. L. and Samelson, R. M. 2006. Normal-mode analysis of a baroclinic wave-mean oscillation. *J. Atmos. Sci.* **63**, 2795–2812.

Yoden, S. and Nomura, M. 1993. Finite time lyapunov stability analysis and its application to atmospheric predictability. *J. Atmos. Sci.* **50**, 1531–1543.